

VIP **Hydrogen Evolution Reaction** Very Important PaperInternational Edition: DOI: 10.1002/anie.201707238
German Edition: DOI: 10.1002/ange.201707238 **Surfactant-Assisted Phase-Selective Synthesis of New Cobalt MOFs and Their Efficient Electrocatalytic Hydrogen Evolution Reaction**Ya-Pan Wu, Wei Zhou, Jun Zhao, Wen-Wen Dong, Ya-Qian Lan, Dong-Sheng Li,*
Chenghua Sun,* and Xianhui Bu*

Abstract: Reported herein are two new polymorphic Co-MOFs (CTGU-5 and -6) that can be selectively crystallized into the pure 2D or 3D net using an anionic or neutral surfactant, respectively. Each polymorph contains a H₂O molecule, but differs dramatically in its bonding to the framework, which in turn affects the crystal structure and electrocatalytic performance for hydrogen evolution reaction (HER). Both experimental and computational studies find that 2D CTGU-5 which has coordinates water and more open access to the cobalt site has higher electrocatalytic activity than CTGU-6 with the lattice water. The integration with co-catalysts, such as acetylene black (AB) leads to a composite material, AB&CTGU-5 (1:4) with very efficient HER catalytic properties among reported MOFs. It exhibits superior HER properties including a very positive onset potential of 18 mV, low Tafel slope of 45 mV dec⁻¹, higher exchange current density of 8.6 × 10⁻⁴ A cm⁻², and long-term stability.

The development of new electrocatalytic materials is of increasing importance because of their critical roles in energy conversion and storage.^[1-3] For hydrogen evolution reaction (HER), a key step in the overall water splitting process, noble-metal-based materials have multiple desirable chemical and electrochemical properties, but their scarcity and high cost leave much to be desired. A constant pursuit in the

catalyst design is to develop low-cost, yet highly stable materials with the highest possible energy efficiency by decreasing the overpotentials often needed to drive the reaction.^[4] Towards these goals, a variety of catalysts have been explored.^[5-7]

As a promising family of catalysts, cobalt-based materials such as CoS₂,^[8] CoP,^[9] and others^[10] have attracted lots of attention for HER applications. Since the early work by Chao and Espenson,^[11] a great progress has been made, demonstrating high activity and stability by cobalt-based materials for HER or OER from water.^[12] The development of metal-organic framework materials (MOFs) promises new opportunities, because of their diverse compositions, versatile structure types, and high porosity.^[13] Several strategies have been reported that use MOFs to improve the electrocatalytic efficiency. One is to couple MOFs with functionally complementary materials. For example, the graphene oxide (GO) incorporated Cu-MOFs composite (GO 8 wt.%) was reported with a high activity for HER.^[14] Another strategy is through MOFs nanosheets which offer advanced features such as rapid mass transport, superior electron transfer, and high percentages of exposed catalytic active surfaces.^[5,16] The effectiveness of this strategy was recently demonstrated by Tang et al.^[16] in ultrathin nanosheets of NiCo bimetal-organic framework.

While cobalt plays a prominent role in the development of various types of electrocatalysts, cobalt-based MOFs have been much less studied for HER. We have been interested in synthesizing new cobalt MOFs with diverse structures and in studying the correlation between their structural properties with electrocatalytic properties and mechanisms. Furthermore, we also study these new cobalt MOFs by combining them with select co-catalysts with complementary properties capable of enhancing the HER catalyst performance. Herein, we report two new polymorphic Co^{II} MOFs and their applications in electrocatalytic HER.

Although surfactants have been extensively studied to effectively regulate the size, shape, and properties of nanocrystals,^[17] the use of surfactants to selectively crystallize MOF polymorphs is much less known.^[18] One highly interesting aspect of this work is the existence of two polymorphs with a strong tendency to crystallize as a mixture, yet they could be selectively crystallized into the pure form by an anionic surfactant and a neutral surfactant, respectively (Figure 1). By tuning the stoichiometric ratio between each MOF and acetylene black (AB) (or graphene), a composite material, AB&CTGU-5 (1:4), was found to have a superior activity for HER in acidic media. Specifically, it exhibits a positive onset potential of 18 mV, low Tafel slope of



[*] Dr. Y.-P. Wu, W. Zhou, Prof. Dr. J. Zhao, Dr. W. W. Dong, Prof. Dr. D.-S. Li

College of Materials and Chemical Engineering, Hubei Provincial Collaborative Innovation Center for New Energy Microgrid, Key Laboratory of Inorganic Nonmetallic Crystalline and Energy Conversion Materials, China Three Gorges University
No. 8, Daxue Road, Yichang, 443002 (China)
E-mail: lidongsheng1@126.com

Dr. Y.-P. Wu, Prof. Dr. Y. Q. Lan
School of Chemistry and Materials Science, Nanjing Normal University
Nanjing 210046 (P. R. China)

Prof. Dr. C. Sun
Department of Chemistry and Biotechnology, Faculty of Science, Engineering and Technology, Swinburne University of Technology
Hawthorn VIC 3122 (Australia)
E-mail: chenghuasun@swin.edu.au

Prof. Dr. X. Bu
Department of Chemistry and Biochemistry
California State University
Long Beach, 1250 Bellflower Boulevard, Long Beach, CA 90840 (USA)
E-mail: xianhui.bu@csulb.edu

 Supporting information and the ORCID identification number(s) for the author(s) of this article can be found under:
 <https://doi.org/10.1002/anie.201707238>.

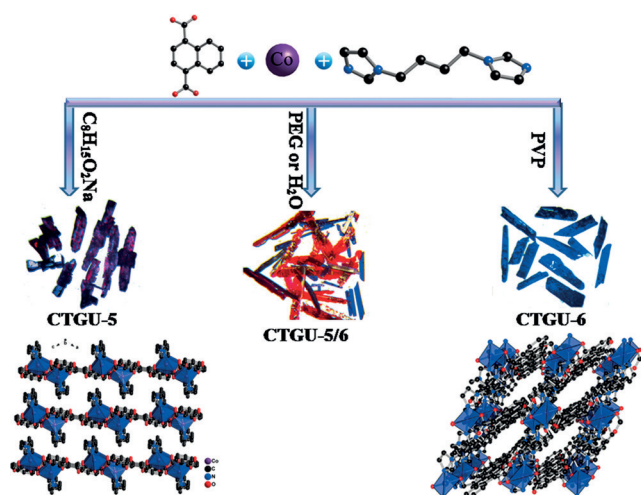


Figure 1. Schematic representation of two isomeric Co MOFs phase-selected by using different surfactants from a mixture of two phases and their crystal structure diagrams.

45 mV dec^{-1} , and high exchange current density of $8.6 \times 10^{-4} \text{ A cm}^{-2}$. The material can maintain a highly stable current density at a constant overpotential of 10 mV for at least 96 h. Such properties make this material among the best MOFs HER catalysts known to date.

Two new polymorphic Co-MOFs, CTGU-5 and CTGU-6, were initially prepared as a mixture. To enable the characterization of their electrocatalytic properties, as well as to probe the correlation of such properties to their crystal structures, extensive synthetic studies were performed, leading to the intriguing discovery that these two phases could be selected by using different surfactants under similar solvothermal systems (see Methods in the Supporting Information for details).

Highly relevant to the catalytic properties is one critical structural difference between CTGU-5 and CTGU-6 involving the coordination mode of water molecule. In CTGU-5, H_2O is coordinated to the Co site, whereas in CTGU-6, H_2O is the lattice molecule only hydrogen-bonded to the framework. Such a difference in the H_2O coordination leads to two very different crystal structures.

Crystal-structure analysis reveals that CTGU-5 has a layered structure in which the Co center adopts distorted octahedral coordination with two O atoms from a chelating carboxylate, one oxygen atom from a non-chelating carboxylate, two mutually *cis* N atoms from two separate N-donor ligands, and finally one water O atom that is *cis* to all other three O atoms (Figure S1a in the Supporting Information). The adjacent Co sites are linked by two dicarboxylate and two 1,4-bis(imidazol)butane ligands to generate a 4-connected square net, further stacked to form a 3D supramolecular architecture (Figure S1b).

In comparison, CTGU-6 features a 3D framework (Figure S2b). The Co center adopts octahedral coordination geometry with four O atoms from two chelating carboxylate groups and two *cis*-N atoms (Figure S2a). CTGU-6 has a 4-connected framework, in which two carboxylate anions and

bib ligands crosslink the Co^{II} atoms to form a 3D four-fold interpenetrated diamond-type network (Figure S2c,d).

The HER catalytic activities of CTGU-5 and CTGU-6 modified glassy carbon (GC) electrodes were evaluated by electrochemical experiments performed in $0.5 \text{ M H}_2\text{SO}_4$ aqueous solution with a scan rate of 5 mV s^{-1} . It should be noted that polarization curves were not corrected for IR compensation. As is well known, the electrode with glassy carbon (GC) shows poor HER activity, on the other hand, Pt/C exhibits a high HER activity with nearly zero onset overpotential (η) and high current density. CTGU-5 and CTGU-6 modified GC can approach a large current density of 10 mA cm^{-2} at an overpotential of 388 and 425 mV as well as positive onset potential of 298 and 349 mV (Figure 2, Table 1, and Table 2), respectively. These small values suggest that CTGU-5 and CTGU-6 have superior HER catalytic activity compared to other reported MOF materials.

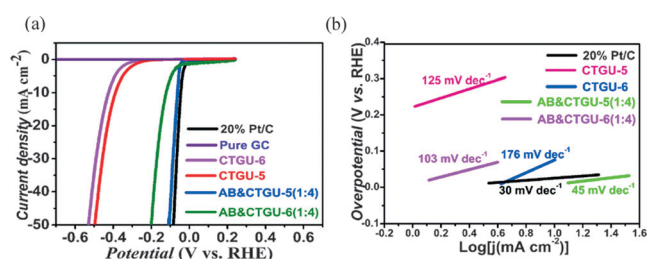


Figure 2. a) Polarization curves for various electrocatalysts in $0.5 \text{ M H}_2\text{SO}_4$ aqueous solution; b) Tafel plots of the corresponding polarization curves.

Table 1: Properties of various CTGU-5 HER catalysts.

Catalyst	Onset Potential [mV]	Tafel slope [mVdec ⁻¹]	η_{10} [mV] ^[a]	j_0 [Acm ⁻²] ^[b]
CTGU-5	298	125	388	1.7×10^{-5}
AB&CTGU-5 (1:8)	181	98	280	3.9×10^{-5}
AB&CTGU-5 (1:4)	18	45	44	8.6×10^{-4}
AB& CTGU-5 (2:4)	21	51	62	3.7×10^{-4}
AB& CTGU-5 (3:4)	43	57	77	2.4×10^{-4}
AB& CTGU-5 (4:4)	26	61	67	3.8×10^{-4}
AB& CTGU-5 (5:4)	45	64	90	1.8×10^{-4}

[a] Represents the overpotential (η). [b] Represents the exchange current density.

Table 2: The catalytic parameters of different HER catalysts.

Catalyst [†]	Onset Potential [mV]	Tafel slope [mVdec ⁻¹]	η_{10} [mV] ^[a]	j_0 [Acm ⁻²] ^[b]	Ref.
20%Pt/C	Ca. 0	30	40	1.7×10^{-4}	–
CTGU-5	298	125	388	1.7×10^{-5}	–
CTGU-6	349	176	425	3.7×10^{-4}	–
Cu-MOFs	202	135	369	3.91×10^{-2}	[14]
NENU-501	304	137	392	2.51×10^{-4}	[15]
NENU-499	45	122	570	4.23×10^{-4}	–
NENU-5	518	94	585	4.90×10^{-4}	–
HKUST-1	612	127	691	5.65×10^{-4}	–

[a] Represents the overpotential (η). [b] Represents the exchange current density.

To understand the HER activities of CTGU-5 and -6, computational studies using density functional theory (DFT) were performed. Using CTGU-5 as an example, as shown in Figure 3a, a pair of proton and electron ($\text{H}^+ + \text{e}^-$) is

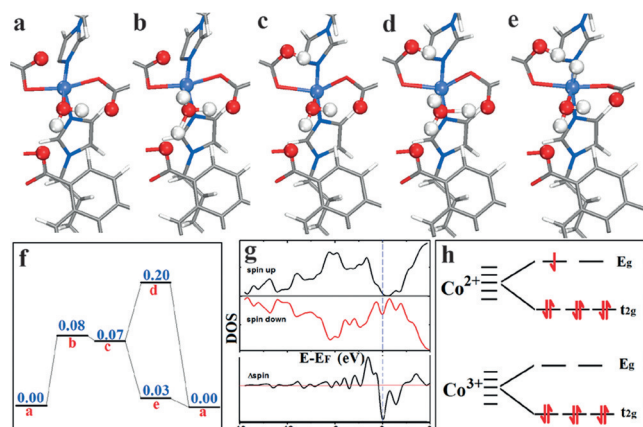


Figure 3. a)–e) Possible steps of the HER process on CTGU-5 surfaces; Co light blue sphere, N blue framework model, O red, H white; see text for details. f) Standard free-energy diagram of the HER process on CTGU-5 surfaces; g) the density of states (DOS) of 2D CTGU-5; h) the valence state of Co-metal in 2D CTGU-5.

introduced to the catalyst with H^+ combining with water to form H_3O^+ (Figure 3b). Then, one hydrogen from H_3O^+ shifts to the neighboring oxygen through hydrogen bonding to form a stable -OH group (Figure 3c). After the first H addition, the second pair of ($\text{H}^+ + \text{e}^-$) is introduced, also forming H_3O^+ . This allows two possible paths to occur, including internal H transfer to form the second -OH group or shifting to the Co site, as shown in Figures 3d and 3e, respectively. To determine the possible path, the energy profile for the full path $a \rightarrow b \rightarrow c \rightarrow d(e) \rightarrow a$ has been obtained (Figure 3f). It shows that $a \rightarrow b \rightarrow c \rightarrow e \rightarrow a$ is favorable with the maximum energy input of 0.08 eV, indicating the HER overpotential is very small (ca. 0.08 V), consistent with experimental data.

To understand the above reaction route, further studies were performed, starting from the density of states (DOS) of 2D CTGU-5 (Figure 3g) with spin up and down. According to this, the initial catalyst shows metallic feature because the Fermi line (Figure 3g; blue dotted line) gets across spin-down states and thus excellent conductivity can be expected. In addition, net spin has also been found from the spin difference Δ_{spin} . This is related to the valence state of Co-metal in the catalyst, and high spin indicates the nature of Co^{2+} , based on the crystal field theory, as shown in Figure 3h, which is confirmed by the XPS result (Figure S7). This is informative because the unpaired electron and empty E_g state can trap proton and electron, respectively, which is the basis for high performance HER catalysts.

To clarify the factors contributing to the HER performance of CTGU-5, the HER activity of pure AB- and graphene-modified electrodes was measured as the reference. For comparison, new composite materials made from CTGU-5 and different conducting materials were also studied (Table 2 and Table S3). As shown in Figure 2, the HER

onset potential for composites-modified electrodes is more positive than that of AB-only modified electrode. The HER onset potential is observed at 298 mV for CTGU-5, and the values decrease steadily after mixing with acetylene black. The best-performing composite, AB:CTGU-5 (1:4), exhibits extraordinary catalytic behavior with a positive onset overpotential of 18 mV and a Tafel slope of 45 mV dec^{-1} . Similarly, when acetylene black (AB) was replaced by graphene, the onset potentials are also decreased (Figure S8), compared with the pure Co^{II} MOFs. With graphene (6 wt %) in CTGU-5, the composite catalyst exhibits an optimal HER activity, with a low onset overpotential of 23 mV and a Tafel slope of 88 mV dec^{-1} . These results demonstrate that the HER activity of our MOFs-based composites benefits from the synergistic effect between Co-MOFs materials and conducting co-catalysts. It is suggested here that CTGU-5 might contribute to the lower overpotential while AB or graphene promotes the current density. Thus, it is beneficial to integrate conducting materials with Co-MOFs, because such integration not only improves the electrical conductivity but also increases the current density.^[19] In forming the composite materials, CTGU-5 with 2D layer has better electrocatalytic properties than CTGU-6 with 3D framework, likely because it better facilitates charge transfer. It is worth noting that AB&CTGU-5 (1:4) exhibits the remarkable HER performance among MOFs materials as evidenced by its very positive onset potential of 18 mV, low Tafel slope of 45 mV dec^{-1} , and long-term stability.

The Tafel slope is an important property of electrocatalytic materials, which is determined by the rate-limiting step of HER. Figure 2b displays the Tafel plots for AB&CTGU-5 composites. For comparison, the Tafel plots for Pt/C, CTGU-5, and CTGU-6 are also shown. The Tafel slopes of 30, 125, 176, 45, and 103 mV dec^{-1} were measured for commercial 20% Pt/C, CTGU-5, CTGU-6, AB&CTGU-5, and AB&CTGU-6 catalysts, respectively. Moreover, as one of the most important measures of HER activity, the exchange current density (j_0), has also been calculated to evaluate the level of performance by the AB&CTGU-5 catalyst (Table 1. Remarkably, the exchange current density of AB&CTGU-5 (1:4) ($8.6 \times 10^{-4} \text{ A cm}^{-2}$) is noticeably larger than that of commercial 20% Pt/C catalyst ($1.7 \times 10^{-4} \text{ A cm}^{-2}$). These results suggest that the superior catalytic activity of AB&CTGU-5 could result from the intimate integration of the two components, leading to increased charge transport and synergistic interactions between the co-catalyst and CTGU-5 (Figure S9). Finally, the Tafel slopes for AB&CTGU-5 show that the HER proceeds by a Volmer-Heyrovsky mechanism. Overall, AB&CTGU-5 shows impressive properties because it has low onset potential and overpotential, small Tafel slope, and high exchange current density.

The physical and morphological characterizations of AB&CTGU-5(1:4) are shown in Figure 4. The laminar structure of the composite can be discerned well by transmission electron microscopy (TEM). Besides, the selected-area electron diffraction (SAED) pattern displays the individual spots associated with concentric rings, indicating the polycrystalline nature of AB&CTGU-5(1:4) (Figure 4b).

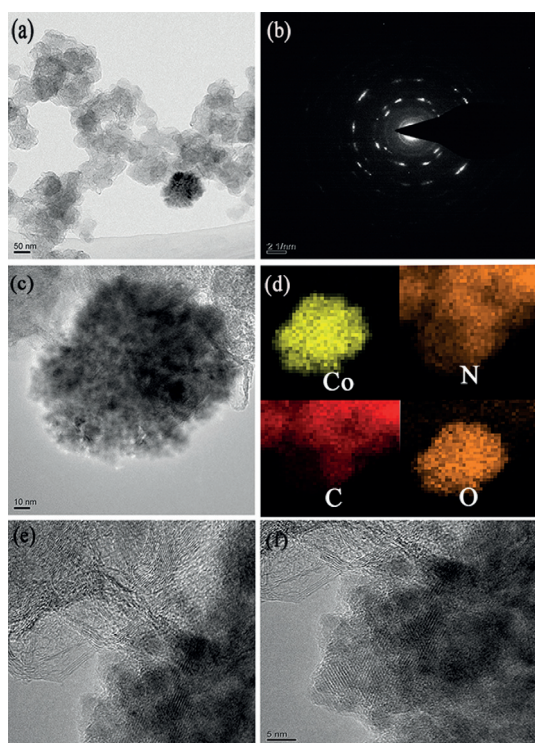


Figure 4. a),c) The TEM image of AB&CTGU-5(1:4); b) the SAED pattern of CTGU-5&AB(1:4); d) TEM-EDS mapping images of AB&CTGU-5(1:4), e),f) the HRTEM image of AB&CTGU-5(1:4).

Elemental mapping has been employed to obtain the elemental distribution of Co, C, N, and O in the composites (Figure 4d), verifying that CTGU-5 particles are embedded in the surface of acetylene black.

The electrochemical impedance spectra (EIS) provide further insight into the electrode kinetics of the studied catalysts (Figure S10). These plots are all composed of a semi-circle at high-frequency regions and a vertical line at low-frequency regions. The charge-transfer resistance (R_{ct}) value of AB&CTGU-5(1:4) is much lower than that of the other three catalysts, which indicates a highly efficient electron transport and favorable HER kinetics at the AB&CTGU-5(1:4) electrolyte interface. Finally, the durability is of crucial importance for practical applications. The long-term stability of AB&CTGU-5 (1:4) shows very limited deterioration of cathodic currents for 96 h. The strong performance could be due to unique scaffold structure of 2D CTGU-5 layers and acetylene black, leading to the outstanding catalytic activity of AB&CTGU-5 (Figure 5).

In summary, two new Co-MOFs were synthesized and selectively separated into the pure form by using an anionic surfactant and neutral surfactant, respectively. Despite similar coordination modes by Co^{II} to ligands, the water molecule in these two MOFs behaves very differently, in coordination mode and lattice mode, in 2D and 3D structures, respectively. Their electrocatalytic applications for HER were studied. The HER electrocatalytic activity of 2D CTGU-5 is distinctly superior to that of the 3D CTGU-6. By systematically varying stoichiometric ratio between MOFs and acetylene black (AB), the composite material shows an improved activity for

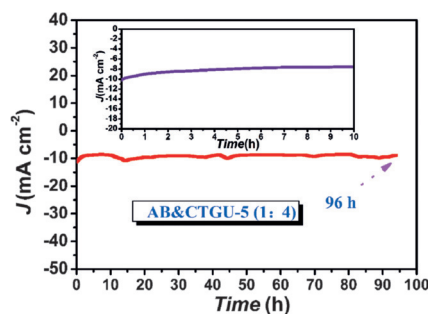


Figure 5. Chronoamperometric profiles of AB&CTGU-5(1:4) in 0.5 M H_2SO_4 at $\eta = -0.25$ V versus RHE.

the hydrogen evolution reaction (HER) in acidic media along with good stability. It is worth noting that AB&CTGU-5(1:4) exhibits the best HER performance among all MOFs materials due to its lower Tafel slope of 45 mV dec^{-1} , high exchange current density of $8.6 \times 10^{-4} \text{ A cm}^{-2}$, and long-term stability. This work establishes for the first time the 2D Co^{II} MOFs and conducting co-catalyst composite as an efficient and stable electrocatalyst for the hydrogen evolution reaction in acid media.

Acknowledgements

This work was supported by the NSF of China (Nos.: 21673127, 21373122, 21671119, 51572152, and 51502155).

Conflict of interest

The authors declare no conflict of interest.

Keywords: cobalt · composite materials · electrocatalysis · hydrogen evolution reaction · MOFs

How to cite: *Angew. Chem. Int. Ed.* **2017**, *56*, 13001–13005
Angew. Chem. **2017**, *129*, 13181–13185

- [1] a) R. D. L. Smith, M. S. Prevot, R. D. Fagan, Z. Zhang, P. A. Sedach, M. K. J. Siu, S. Trudel, C. P. Berlinguette, *Science* **2013**, *340*, 60–63; b) H. Yin, S. Zhao, K. Zhao, A. Muqsit, H. Tang, L. Chang, H. Zhao, Y. Gao, Z. Tang, *Nat. Commun.* **2015**, *6*, 6430.
- [2] a) M. D. Symes, L. Cronin, *Nat. Chem.* **2013**, *14*, 404–409; b) S. W. Sheehan, J. M. Thomsen, U. Hintermair, R. H. Crabtree, G. W. Brudvig, C. A. Schmuttenmaer, *Nat. Commun.* **2015**, *6*, 6469.
- [3] a) I. Roger, M. A. Shipman, M. D. Symes, *Nat. Rev. Chem.* **2017**, <https://doi.org/10.1038/s41570-016-0003>; b) J. S. Li, Y. Wang, C. H. Liu, S. L. Li, Y. G. Wang, L. Z. Dong, Z. H. Dai, Y. F. Li, Y. Q. Lan, *Nat. Commun.* **2016**, *7*, 11204.
- [4] a) X. Ma, K. Zhao, H. Tang, Y. Chen, C. Lu, W. Liu, Y. Gao, H. Zhao, Z. Tang, *Small* **2014**, *10*, 4664–4670; b) Y. Jiao, Y. Zheng, M. Jaroniec, S. Z. Qiao, *Chem. Soc. Rev.* **2015**, *44*, 2060–2086.
- [5] W. Wang, X. Xu, W. Zhou, Z. Shao, *Adv. Sci.* **2017**, *4*, 1600371.
- [6] a) K. N. Ferreira, T. M. Iverson, K. Maghlaoui, J. Barber, S. Iwata, *Science* **2004**, *303*, 1831–1838; b) M. W. Kanan, D. G. Nocera, *Science* **2008**, *321*, 1072–1075; c) J. Suntivich, K. J. May, H. A. Gasteiger, J. B. Goodenough, Y. Shao-Horn, *Science* **2011**, *334*, 1383–1385; d) Y. Y. Ma, C. X. Wu, X. J. Feng, H. Q. Tan,

- L. K. Yan, Y. Liu, Z. H. Kang, E. B. Wang, Y. G. Li, *Energy Environ. Sci.* **2017**, *10*, 788–798.
- [7] J. Wang, F. Xu, H. Jin, Y. Chen, Y. Wang, *Adv. Mater.* **2017**, *29*, 1605838.
- [8] a) D. Kong, J. J. Cha, H. Wang, H. R. Lee, Y. Cui, *Energy Environ. Sci.* **2013**, *6*, 3553–3558; b) S. Peng, L. Li, X. Han, W. Sun, M. Srinivasan, S. G. Mhaisalkar, F. Cheng, Q. Yan, J. Chen, S. Ramakrishna, *Angew. Chem. Int. Ed.* **2014**, *53*, 12594–12599; *Angew. Chem.* **2014**, *126*, 12802–12807; c) M. S. Faber, R. Dziedzic, M. A. Lukowski, N. S. Kaiser, Q. Ding, S. Jin, *J. Am. Chem. Soc.* **2014**, *136*, 10053–10061.
- [9] a) H. Du, Q. Liu, N. Cheng, A. M. Asiri, X. Sun, C. M. Li, *J. Mater. Chem. A* **2014**, *2*, 14812–14816; b) E. J. Popczun, C. G. Read, C. W. Roske, N. S. Lewis, R. E. Schaak, *Angew. Chem. Int. Ed.* **2014**, *53*, 5427–5430; *Angew. Chem.* **2014**, *126*, 5531–5534.
- [10] a) H. Fei, J. Dong, M. J. Arellano-Jiménez, G. Ye, N. D. Kim, E. L. G. Samuel, Z. Peng, Z. Zhu, F. Qin, J. Bao, M. J. Yacaman, P. M. Ajayan, D. Chen, J. M. Tour, *Nat. Commun.* **2015**, *6*, 8668; b) X. Zou, Y. Zhang, *Chem. Soc. Rev.* **2015**, *44*, 5148–5180.
- [11] T. H. Chao, J. H. Espenson, *J. Am. Chem. Soc.* **1978**, *100*, 129–133.
- [12] a) X. L. Hu, B. S. Brunshwing, J. C. Peters, *J. Am. Chem. Soc.* **2007**, *129*, 8988–8998; b) P. A. Jacques, V. Artero, J. Pecaut, M. Fontecave, *Proc. Natl. Acad. Sci. USA* **2009**, *106*, 20627–20632; c) S. Friedle, E. Reisner, S. J. Lippard, *Chem. Soc. Rev.* **2010**, *39*, 2768–2779; d) N. M. Muresan, J. Willkomm, D. Mersch, Y. Vaynzof, E. Reisner, *Angew. Chem. Int. Ed.* **2012**, *51*, 12749–12753; *Angew. Chem.* **2012**, *124*, 12921–12925; e) E. S. Andreiadis, P. A. Jacques, P. D. Tran, A. Leyris, M. C. Kerlidou, B. Jousset, M. Matheron, J. Pecaut, S. Palacin, M. Fontecave, V. Artero, *Nat. Chem.* **2012**, *5*, 48–53; f) S. Zhao, H. Yin, L. Du, L. He, K. Zhao, L. Chang, G. Yin, H. Zhao, S. Liu, Z. Tang, *ACS Nano* **2014**, *8*, 12660–12668; g) P. Manna, J. Debgupta, S. Bose, S. K. Das, *Angew. Chem. Int. Ed.* **2016**, *55*, 2425–2430; *Angew. Chem.* **2016**, *128*, 2471–2476.
- [13] A. Morozan, F. Jaouen, *Energy Environ. Sci.* **2012**, *5*, 9269–9290.
- [14] M. Jahan, Z. Liu, K. P. Loh, *Adv. Funct. Mater.* **2013**, *23*, 5363–5372.
- [15] J. S. Qin, D. Y. Du, W. Guan, X. J. Bo, Y. Li, L. Guo, Z. M. Su, Y. Y. Wang, Y. Q. Lan, H. C. Zhou, *J. Am. Chem. Soc.* **2015**, *137*, 7196–7197.
- [16] S. Zhao, Y. Wang, J. Dong, C. T. He, H. Yin, P. An, K. Zhao, X. Zhang, C. Gao, L. Zhang, J. Lv, J. Wang, J. Zhang, A. M. Khattak, N. A. Khan, Z. Wei, J. Zhang, S. Liu, H. Zhao, Z. Tang, *Nat. Energy* **2016**, *1*, 16184.
- [17] a) W. W. Xiong, J. Miao, K. Ye, Y. Wang, B. Liu, Q. Zhang, *Angew. Chem. Int. Ed.* **2015**, *54*, 546–550; *Angew. Chem.* **2015**, *127*, 556–560; b) W. W. Xiong, Q. Zhang, *Angew. Chem. Int. Ed.* **2015**, *54*, 11616–11623; *Angew. Chem.* **2015**, *127*, 11780–11788; c) G. Liu, J. Liu, L. Nie, R. Ban, G. Armatas, X. T. Tao, Q. Zhang, *Inorg. Chem.* **2017**, *56*, 5498–5501.
- [18] a) J. Gao, K. Ye, M. He, W. W. Xiong, W. Cao, Z. Y. Lee, Y. Wang, T. Wu, F. Huo, X. Liu, Q. Zhang, *J. Solid State Chem.* **2013**, *206*, 27–31; b) J. Zhao, Y. Wang, W. Dong, Y. Wu, D. Li, B. Liu, Q. Zhang, *Chem. Commun.* **2015**, *51*, 9479–9482.
- [19] A. J. Clough, J. W. Yoo, M. H. Mecklenburg, S. C. Marinescu, *J. Am. Chem. Soc.* **2015**, *137*, 118–121.

Manuscript received: July 17, 2017

Accepted manuscript online: August 1, 2017

Version of record online: August 18, 2017